Analysis of Experimental Data for Polystyrene Orientation during Stress Relaxation Using Semigrand Canonical Monte Carlo Simulation

Frederick L. Colhoun, Robert C. Armstrong, and Gregory C. Rutledge*

Department of Chemical Engineering, Massachusetts Institute of Technology, Cambridge, Massachusetts 02139

Received March 6, 2002; Revised Manuscript Received May 9, 2002

ABSTRACT: Monte Carlo simulation in the semigrand canonical ensemble is used to construct molecular models of atactic polystyrene samples that are quenched in nonequilibrium states at various times following the cessation of steady shear flow. Experimental data collected by slow magic angle spinning DECODER NMR on quenched, oriented samples prescribe a measure of the residual orientation of chain repeat units after shear and its subsequent decay with time. By speciating the system in orientation space, a series of semigrand canonical Monte Carlo simulations describe the detailed molecular conformational changes that occur in stress relaxation over the time scale of seconds and minutes. The general method of reconstructing molecular conformations from orientation data is also illustrated with several test cases using simple chain models.

Introduction

Quantification of the microstructure of a polymeric material is important due to the influence it exerts on the macroscopic physical properties of that material.[1] Accurate molecular simulation of that microstructure enables the calculation of thermomechanical and optical material properties. Methods for the simulation of polymeric systems in thermodynamic equilibrium are well established. Recently, attention has been devoted to the simulation of systems in nonequilibrium states. In these systems, ensembles of polymer chains exist in configurations that are deformed relative to the random-coil representation of equilibrium structures. Of particular interest is the ability to incorporate experimentally determined orientation information at some length scale into molecular simulations. This would allow the properties of oriented (nonequilibrium) systems to be simulated.

Broadly speaking, two classes of simulation methods exist: deterministic and stochastic. Molecular dynamics (MD) is a deterministic method that invokes Newton's equation of motion to simulate the realistic dynamics of a molecular system, including the evolution of a system under the influence of external, applied forces, such as a shear or extensional force (nonequilibrium molecular dynamics, NEMD). Monte Carlo (MC) is a stochastic method that normally does not provide any information regarding dynamical behavior but can be used to simulate the structure and properties of a molecular system at thermodynamic equilibrium without regard to the time scale required to equilibrate the system. Brownian dynamics augments the deterministic MD equations with a stochastic force to simulate realistic dynamics for the "slower" degrees of freedom under the influence of collisions with smaller, faster objects in the system. Nonetheless, both molecular dynamics simulation and Brownian dynamics simulation (with hydrodynamic interactions)[2−6] for time scales longer than the order of nanoseconds are beyond most computing capabilities. Here, we investigate the use of Monte Carlo simulation to simulate the structure of a molecular system constrained to lie far from equilibrium. The constraint is chosen to reflect the out-of-equilibrium nature of the system and results in the simulation of a *local* equilibrium state. By performing a series of simulations in which the constraint changes on a time scale that is long compared to that accessible by MD, e.g., comparable to the slower dynamical modes (ν < 1 MHz) of a polymeric system, the structural evolution of a system may be studied by either MD or MC; in particular, the quasi-static evolution of the ensemble over long time scales, rather than the short time dynamics of individual chains, is followed. Experimental data offer one means for quantifying the deviation from equilibrium for a molecular system and provide information implicitly on the constraints operative on a collection of molecules over a short period of time (the duration of the data collection).

The generation of ensembles that correctly reproduce known experimental data is one of a class of "inverse problems" and has been pursued in several ways. Traditionally, a standard Metropolis MC technique is employed with an assumed force field. Simulations are performed, and the properties predicted are subsequently compared with experimental data collected on those properties.[7−9] If the predictions are in agreement with the data, then the force field is judged satisfactory and used in subsequent studies. If not, then the force field is exchanged or modified in an effort to obtain agreement. The data used to fit force fields are typically limited to that collected at equilibrium; otherwise, the force field parametrization itself would biased by the external potential and would have difficulty in predicting equilibrium properties correctly.

A second approach is reverse Monte Carlo (RMC).[10] In this method, the physically based force field is discarded in favor of a statistical measure of how well the features of a particular configuration reproduce the experimental observations. Hence, the experimental data solely dictate the acceptance of any given MC move. If a move brings the ensemble into closer agreement with the data, it is accepted; if the move worsens the agreement with the data, it is rejected with a certain probability.[11−13]

* To whom correspondence should be addressed.

10.1021/ma020347h CCC: $22.00
Published on Web 06/19/2002

A third approach is the use of a semigrand canonical Monte Carlo (SGMC) simulation that incorporates experimental data into a thermodynamic simulation by defining the (polydisperse) species in a system according to their contribution to the intensity of an experimental measurement, rather than according to their chemical identities. This method has been verified previously to reproduce a predetermined radial distribution function for the Lennard-Jones fluid.[14] In the absence of an external potential, the resulting activities can be related to the underlying interatomic potential. For systems in which the interatomic potential is known from equilibrium information, the resulting activities can be related to an effective constraint potential when the system is out of equilibrium.

This paper demonstrates the use of the SGMC method to describe single-chain molecular conformations during relaxation of a polymer melt after shearing. Experimental data in the form of orientation distribution functions were obtained by ^{13}C SMAS-DECODER NMR measurements on a series of sheared polystyrene samples. Each sample was quenched in the glassy state after being allowed to relax in the melt state for a period of time after shearing. Accordingly, these data can reflect conformational changes during polymer relaxation on the time scale of seconds, minutes, and even hours. The use of experimental data in a simulation is combined with available semiempirical force fields in a thermodynamically consistent manner. Thus, within a quasistatic approximation, this method enables much longer time scales to be studied with molecular simulation methods than was previously possible.

Theory

The current method employs the SGMC formalism developed by Rutledge,[14] based on the statistical thermodynamics of polydisperse fluids,[15] for the inclusion of an orientational potential in a single-chain Monte Carlo simulation. In general, the intermolecular potential ϕ_{ij} between two interacting beads depends on the positions (r_i, r_j) and species types (I_i, I_j) of the beads:

$$\phi_{ij} = \phi(\{r_i,I_i\},\{r_j,I_j\}) \tag{1}$$

Even if the beads are *chemically* identical, the beads may be differentiated from one another according to some other variable, such as the orientation of a vector designating the backbone direction of the polymer chain at each bead. This change in speciation of the system merely changes it from nominally a single-component system to a multicomponent system. If the new variable used to distinguish bead types is continuously distributed, then the system is said to be polydisperse, with the probability distribution (i.e., composition) of bead types obeying the following normalization:

$$\int_{-\infty}^{\infty} p(I)\, \mathrm{d}I = 1; \quad p(I) \geq 0 \tag{2}$$

When the total number of beads is held fixed, as in the canonical ensemble, the resulting polydisperse system is simulated analogously in the semigrand canonical ensemble. This change allows the incorporation of orientation information into the calculation of the conformational energy, which is central to the simulation method. We define an orientational activity $a(I)$, where I is a measure of orientation; e.g., $I_i = \cos\theta_i$ and θ_i is the angle between the backbone of the chain at bead i and the sample director. The corresponding excess orientation potential is

$$\mu_{\mathrm{ex}}(I_i) = \beta \ln(a(I_i)) \tag{3}$$

Simulation is carried out at constant N,V,T, and $\{a_i/a_{\mathrm{ref}}\}$. The semigrand canonical partition function in the polydisperse limit is[15]

$$Y = \frac{1}{N!}\int_{I_1}\cdots\int_{I_N} Z_N q^N \left[\prod_{i=1}^{N}\frac{a(I_i)}{a_{\mathrm{ref}}}\right]\prod_{i=1}^{N}\mathrm{d}I_i \tag{4}$$

where N is the number of beads, β is the Boltzmann factor $1/kT$, $a(I)$ is the activity of a bead whose orientation is I, a_{ref} is the activity of a bead in the reference orientation, q is the internal partition function for a bead (which does not depend on I in this case), and Z_N is the canonical partition function:

$$Z_N = \int_{r_1}\cdots\int_{r_N} \mathrm{e}^{-\beta U}\prod_{i=1}^{N}\mathrm{d}r_i \tag{5}$$

where U is the potential energy:

$$U = \frac{1}{2}\sum_i\sum_j \phi_{ij} \tag{6}$$

Thus, the probability of obtaining a bead in state I is

$$p(I) = \frac{1}{\mathrm{Y}}\int_{I_2}\cdots\int_{I_N} \frac{Z_N q^N}{N!}\left[\prod_{i=1}^{N}\frac{a(I_i)}{a_{\mathrm{ref}}}\right]\prod_{i=2}^{N}\mathrm{d}I_i \tag{7}$$

The condition of microscopic reversibility for the generation of a Markov process for the orientational part of the problem is

$$p(\{r_i,I_i\}_k)w(k \rightarrow l) = p(\{r_i,I_i\}_l)w(l \rightarrow k) \tag{8}$$

$p(\{r_i,I_i\}_k)$ is the a priori probability that a state k exists wherein for each bead i the location and orientation of the bead are r_i and I_i, respectively. $w(k \rightarrow l)$ is the transition probability from state k to state l. With the definition of the residual activity for orientation I (which is assumed here not to depend on bead position r)

$$a^*(I) = \frac{a(I)\, q(I)}{p(I)} \tag{9}$$

the Metropolis criterion for acceptance of a new conformation becomes

$$rn[0,1) < \min\left\{1, \prod_{i=1}^{N}\frac{[a^*(I_i)\, p(I_i)]_{\mathrm{new}}}{[a^*(I_i)\, p(I_i)]_{\mathrm{old}}} \exp(-\beta(U_{\mathrm{new}} - U_{\mathrm{old}}))\right\} \tag{10}$$

In the evaluation of this expression, the value of $p(I)$ is known, but there is no way to know the residual activity profile a priori. Therefore, the residual activity profile can be obtained in an iterative manner according to

$$a^*_{\mathrm{new}}(I) = a^*_{\mathrm{old}}(I)\left[\left(\frac{p(I)}{p(I_0)}\right)^{\mathrm{target}}\left(\frac{p(I_0)}{p(I)}\right)^{\mathrm{calc}}\right] \tag{11}$$

In this expression, the "calculated" values are taken from the Monte Carlo representation of the experimental distribution function, whereas the "target" values are obtained by evaluating the distribution function implied by the experimental data. If the distributed variable is one of orientation, the logical reference state I_0 taken for these calculations is the axis of orientation. For the initial iteration, we select $a^*(I) = 1$, although other choices are possible. For further details regarding the SGMC method, the reader is referred to ref 14.

In two limiting cases, the calculation of the residual activity profiles may be simplified. If the target $p(I)$ is independent of I (i.e., the system is isotropic) or if the orientation I of any bead is independent of the orientations of the other beads in the system, then $a^*(I) = a_{\mathrm{ref}} = 1$; in the first instance, one recovers the conventional Metropolis MC procedure without constraint, whereas in the second instance, one obtains a simulation which samples the desired distribution $p(I)$ without need for iteration on $a(I)$.

Model Calculations

Prior to applying the SGMC method to real data, we first illustrate its ability to reproduce predetermined uniaxial bond orientation distributions in model chains with different degrees of intramolecular correlation. In these examples, I is the polar orientation angle ($\cos\Theta$) of the chain segments with respect to the global director, the z-axis. The simplest model of a polymer chain is the freely jointed chain or random walk; for simplicity, we assume a bond length of 1 in this illustration. With respect to $p(\cos\Theta)$, the freely jointed chain is ideal; Z_N = constant, and the orientation of each bond in the chain is independent of the orientation of all other bonds. Thus, $a^*(\cos\Theta) = 1$ regardless of the target $p(\cos\Theta)$, and the desired ensemble can be simulated immediately based on knowledge of the target $p(\cos\Theta)$ alone. A second, slightly more complicated model commonly employed for polymers is the freely rotating chain, in which the angle formed by successive bonds in the chain is constrained to a particular value (here, we report results for a bond angle of 150°). For this model the orientation of the individual bonds is no longer independent of the other bonds, and $a^*(\cos\Theta)$ must be determined iteratively.

Freely jointed and freely rotating chains of length 20 bonds were simulated by using a generalized reptation algorithm in which 1 to n_r bonds at one end of the chain are removed and regrown at either end of the chain. The chain ends selected for deletion and regrowth were chosen at random to maintain microreversibility. n_r = 3 was found to sample configuration space most efficiently. Each simulation typically entailed 10^5-10^7 Monte Carlo moves. For testing purposes, analytical a priori bond orientation distributions were taken to be of the form $p_{t\mathrm{arget}}(\cos\Theta) = \sum(1/4\pi)c_{2i}P_{2i}(\cos\Theta)$, where the $P_{2i}(\cos\Theta)$ are even-order Legendre polynomials. The distributions were normalized such that $c_0 = 1$. The reference state I_0 was $\cos\Theta = 1$. Figure 1 illustrates the resulting residual activity distributions, $a^*(\cos\Theta)$, for three a priori bond orientation distributions: (i) $c_{2i} = 0$ for $i > 0$ (the isotropic distribution, $\langle P_{2,z}\rangle = 0.0$); (ii) $c_2 = 2$, $c_{2i} = 0$ for $i > 1$ ($\langle P_{2,z}\rangle = 0.4$); (iii) $c_{2i} = 10/3$, 24/11, and 16/33 for $i = 1$, 2, and 3, respectively, $c_{2i} = 0$ for $i > 3$ ($\langle P_{2,z}\rangle = 0.6667$). When the orientation distribution is isotropic, there is no orientational bias, and the simulation reverts to the standard, thermodynamic equilibrium case. In each case, the distribution is cylindrically symmetric, $\langle P_{2,x}\rangle = \langle P_{2,y}\rangle = -\langle P_{2,z}\rangle/2$. By simulation, each of the $\langle P_{2,i=x,y,z}\rangle$ was obtained accurate to four significant figures. Imposition of an anisotropic bond orientation distribution implies a work of orientation and deviation from the distribution of chain conformations at equilibrium. Distortion of chain conformations was quantified using the scaled, mean-square end-to-end distance $\langle R^2\rangle/n$ and the average asphericity, $\langle b\rangle = \langle s_{zz}{}^2\rangle - (\langle s_{xx}{}^2\rangle + \langle s_{yy}{}^2\rangle)/2$, where $s_{ii}{}^2$ is the ith component of the radius of gyration tensor in its principal axis frame for a single chain. For the freely jointed chain, $\langle R^2\rangle/n = 1.0$ for all three distributions, as it should; anisotropy merely results in random walks in lower dimensional spaces. For the freely rotating chain, $\langle R^2\rangle/n$ takes values of 9.4, 12.9, and 15.9 for distributions (i), (ii), and (iii), respectively. The corresponding asphericities $\langle b\rangle$ for the freely jointed chain were 0.000, 0.070, and 0.117 for distributions (i), (ii), and (iii), respectively, and 0.02, 0.86, and 1.00 for the freely rotating chain.

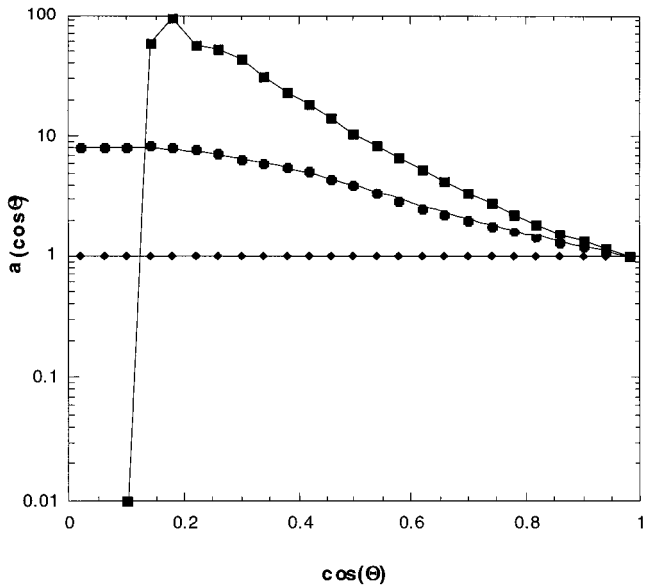

Figure 1. Residual activity profiles for the freely jointed and freely rotating (bond angle = 30°) chain models for three bond orientation distributions. All plots are symmetrical about cos Θ = 0°. Diamonds: freely jointed chain model with any orientation distribution, or isotropic orientation distribution for any chain model. Circles: freely rotating chain with $\langle P_2\rangle = 0.4$. Squares: freely rotating chain with $\langle P_2\rangle = 0.67$ (see text for details).

The change in conformation is also apparent in the intramolecular orientational correlation function, $S(r) = [3\langle\cos^2\eta(r)\rangle - 1]/2$. Here, r is the distance between the centers of two vectors that connect next-nearest neighbor atoms along the chain, and $\eta(r)$ is the angle formed by the two vectors.[16] This is illustrated in Figure 2 for the freely jointed chain, where the correlation function is weighted by the pair distribution function $g(r)$ and plotted against r. The effect of increasing alignment of bonds is clearly manifested in more pronounced correlation peaks in $S(r)g(r)$, peak shifts toward larger r, and correlation out to higher peak order. All of these features are consistent with increased extension of the chain. Significantly, the imposed distribution, combined with the requirements of chain connectivity, also places restrictions on conformational characteristics such as the distribution of torsion angles along the chain. This additional information can be read

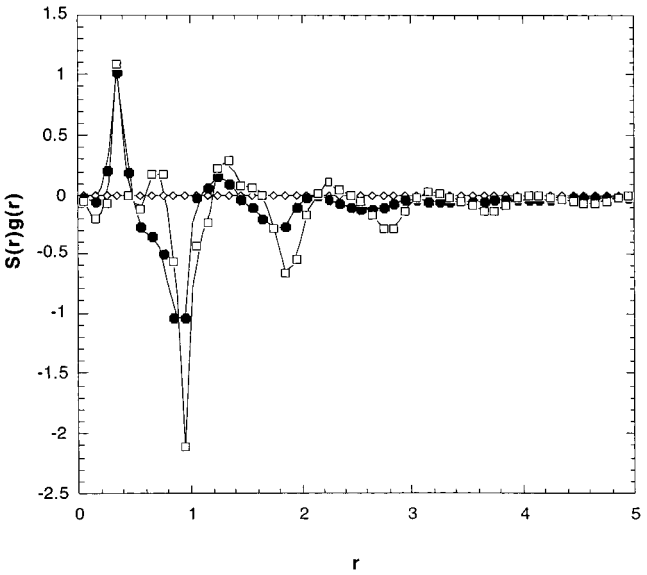

Figure 2. Pair distribution-weighted intramolecular orientational correlation function, $S(r)g(r)$, for freely jointed chains. Here, r is the distance between the centers of mass of two segments, each spanning two consecutive bonds on the same chain. $g(r)$ is the radial distribution function, and $S(r)$ is defined in the text. Diamonds: isotropic bond orientation distribution, $\langle P_2 \rangle = 0.0$. Circles: $\langle P_2 \rangle = 0.4$. Squares: $\langle P_2 \rangle = 0.67$.

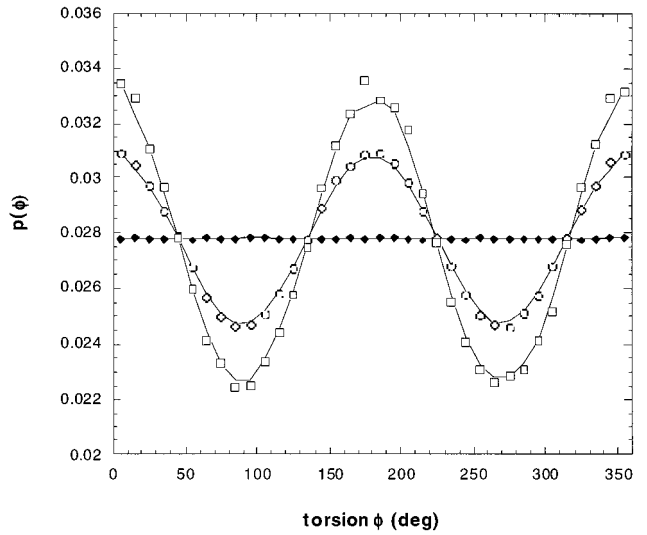

Figure 3. Distribution of torsion angle ϕ for freely jointed chains subject to bond orientation: filled diamonds, isotropic bond orientation distribution, $\langle P_2 \rangle = 0.0$; circles, $\langle P_2 \rangle = 0.4$; squares, $\langle P_2 \rangle = 0.67$. Curves are drawn as visual guides.

from the simulation. As illustrated in Figure 3, increasing orientation of bonds in the freely jointed chain implies an increasing propensity for cis and trans torsion angles.

More realistic polyethylene chain models with hindered rotation potentials and excluded-volume interactions obtained from ref 16 (i.e., $Z_N \neq 1$) have also been simulated. Similar effects are seen in $S(r)$ as well as quantifiable distortion of the torsion angle distribution. The simulation of polystyrene chains which follows below, however, describes the most realistic application of the SGMC method to date.

Simulation of Polystyrene

Conformational Energy Model. We now shift our attention to the simulation of polystyrene chains with realistic intramolecular structure coupled with the use of real experimental data. This case is somewhat more complex than the model systems just described, in that it involves nontrivial torsional and other intra- and intermolecular potentials. In particular, we are concerned here with the conformational changes of polystyrene observed during stress relaxation. We must first select an appropriate force field that will accurately reproduce the isotropic system. Several force fields have been used previously for polystyrene.[17−20] These differ in how they treat various components of the potential energy, such as the bond stretching, bond angle bending, bond torsion, Coulombic, and nonbonded energies as well as in the model compound or molecular segment used to estimate the necessary force field parameters. Table 1 summarizes the principal differences in these force fields. These force fields result in potential energy surfaces which differ in the number and location of the energy minima in torsion space. In particular, inclusion of a Coulombic potential by Rapold and Suter[19] eliminates the energy minimum found by Yoon et al.[17] for the tt conformation of the meso dyad.

The model of Rapold and Suter (RS)[19] was selected for this analysis for several reasons. First, the fixed bond lengths and bond angles make the model less computationally intensive than that of Smith et al.[20] without sacrificing accuracy. Second, the inclusion of electrostatic interactions makes this model preferable to the Mondello models[18] since the phenyl ring of polystyrene is a highly polarized moiety. Finally, the RS model reports the potential energy of 2,4-diphenylpentane (a small molecule analogue of polystyrene) as a function of the two torsional angles ϕ_i and ϕ_{i+1} shown in Figure 4, with the rings rotated to minimize the energy for each conformer. This simplifies the computation of the conformational energy of a polystyrene chain tremendously. It is necessary only to account for the backbone atoms; calculation of the nonbonded and electrostatic energies is avoided since they are included in the potential energy surfaces reported in ref 19.

Contour plots of the conformational energy of the racemo and meso dyads of 2,4-diphenylpentane from[19] are reproduced in Figure 5.[21] We discretized the conformational energy in 5° increments of ϕ, although analytic representations of the conformational energy may also be implemented. All energies are reported in kJ/mol relative to the racemo-tt minimum. The contour intervals are 5 kJ/mol, and the maximum contour value is 45 kJ/mol. The locations and values of the energy minima are given in Table 2. High-energy minima of the $t\bar{g}$ conformations of both dyads were excluded from this analysis since their Boltzmann probabilities at 300 K were at most only 2.9×10^{-6}, and thus these conformations are insignificant.

Since the energy model treats the bond lengths and bond angles as fixed, the conformations of the polymer chains in the simulation are defined solely by the internal torsional angles. Once the first chain of the ensemble is constructed, configuration space is sampled by using an end reptation move, similar to that used for the model chains. However, tacticity of the polystyrene chain imparts some additional complexity to the specification of a chain regrowth or reptation move, and conditional probability distributions are used to improve the selection of trial states for successive torsions which exhibit second-order interactions with their preceding

Table 1. Comparison of Polystyrene Energy Models

model	Yoon[a]	Mondello[b]	Mondello[b]	Smith[c]	Rapold[d]
molecule	PS dyad	all atom PS	united atom PS	2,4-DPP	2,4-DPP
bond length	constant	constant	constant	variable	constant
bond angle	constant	variable	variable	variable	constant
backbone torsion	3-fold	3-fold	3-fold	3-fold	3-fold
phenyl torsion	fixed	isotropic	yes	2-fold	6-fold
Coulombic	not specified	no	no	yes	yes
nonbonded[e]	LJ 6−12	LJ 6−12	LJ 6−12	exp 6	LJ 6−12

[a] From ref 17. [b] From ref 18. [c] From ref 20. [d] From ref 19. [e] LJ 6−12 indicates the Lennard-Jones form for the nonbonded potential, while exp-6 indicates the softer, exponential repulsion term is used instead of $1/r^{12}$.

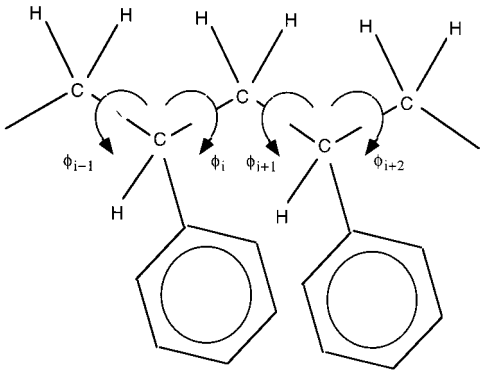

Figure 4. Illustration of the meso dyad of a polystyrene chain in the all-trans conformation. Adapted from ref 19.

torsions. We take these new aspects into account as follows.

First, one must specify the stereochemistry of any new segments added to the chain, such that the overall tacticity does not stray from the desired values during the simulation. When a new bond is formed, the tacticity (meso or racemo) of the resulting dyad is chosen according to Bernoullian statistics, based on the input value of the fraction of meso dyads. The skeletal bond to be grown is thus specified as d or l.[23] Once the stereochemistry of the new bonds to be formed is specified, it would suffice in principle to choose at random the values for each of the torsion angles between 0 and 2π and then accept or reject the new chain based on the Metropolis criterion by using the difference in torsion energy between the new chain and the old. However, for reptative moves in which two or more dyads, or four or more skeletal bonds, are regrown at once, we found this approach to be plagued by poor acceptance rates.

Instead, we select values of the torsion angles according to their probability distribution using the rejection method, which we can then accept with unit probability with respect to torsion energy. In this method, energetically favored torsion angles are selected proportionally more often than high-energy torsion angles. However, because of second-order interactions between successive torsion angles along the chain, it is necessary to account for the state of the preceding torsion in the chain when selecting the value of the next torsion. This is accomplished through the use of conditional probability distributions and is described in detail in Appendix A.

The vector between the two methylene groups on either side of the substituted carbon is used to define the local chain direction at each repeat unit during a simulation and is used to construct the simulated orientational probability distribution. The backbone carbon−carbon bond length is 1.53 Å. The $C-C_p-C$ bond angle (centered on the substituted carbon) is 112°, while the C_p-C-C_p bond angle is 114°.

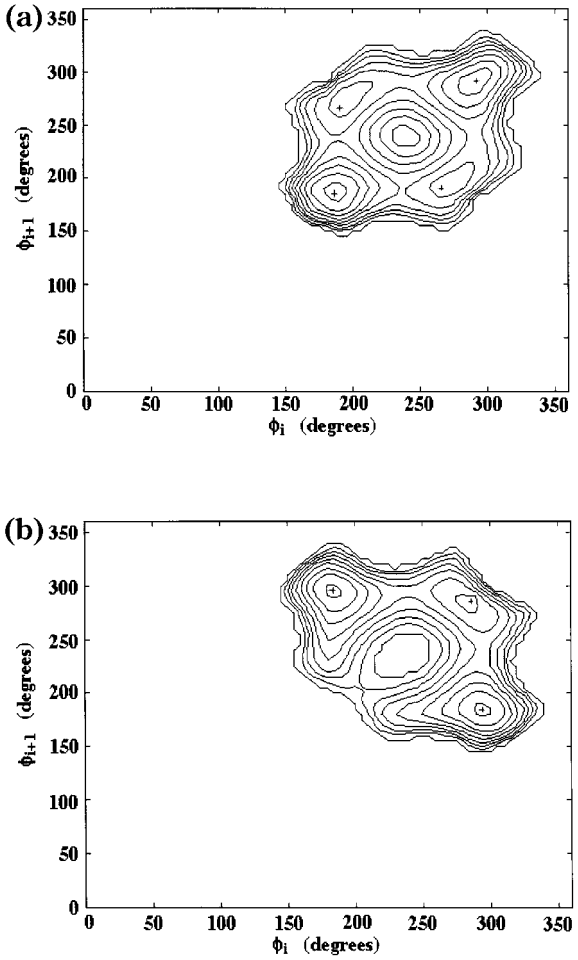

Figure 5. Conformational energy $U(\phi_i,\phi_{i+1})$ contours of the (a) racemo and (b) meso dyad of 2,4-diphenylpentane as a function of the torsion angles. Adapted from ref 19. Contours are spaced every 5 kJ/mol to a maximum of 45 kJ/mol. Values of minima are given in Table 2.

Table 2. Locations and Energies of Minima in Conformation Energy for Racemo and Meso Dyads of 2,4-Diphenylpentane[a]

dyad	conformation	ϕ_i (deg)	ϕ_{i+1} (deg)	energy (kJ/mol)
racemo	tt	5	5	0.0
racemo	tg, gt	10	95	16.4
racemo	gg	115	115	5.9
meso	tg, gt	5	115	3.9
meso	gg	105	105	14.4

[a] All energies are reported relative to the racemo-tt minimum.

Application to Oriented Polystyrene Data. The direction of the chain backbone at each repeat unit in a polystyrene chain is reasonably well approximated by the normal to the phenyl ring on every second carbon.[7] Orientation distributions for the phenyl ring normal were obtained from the analysis of ^{13}C SMAS DE-

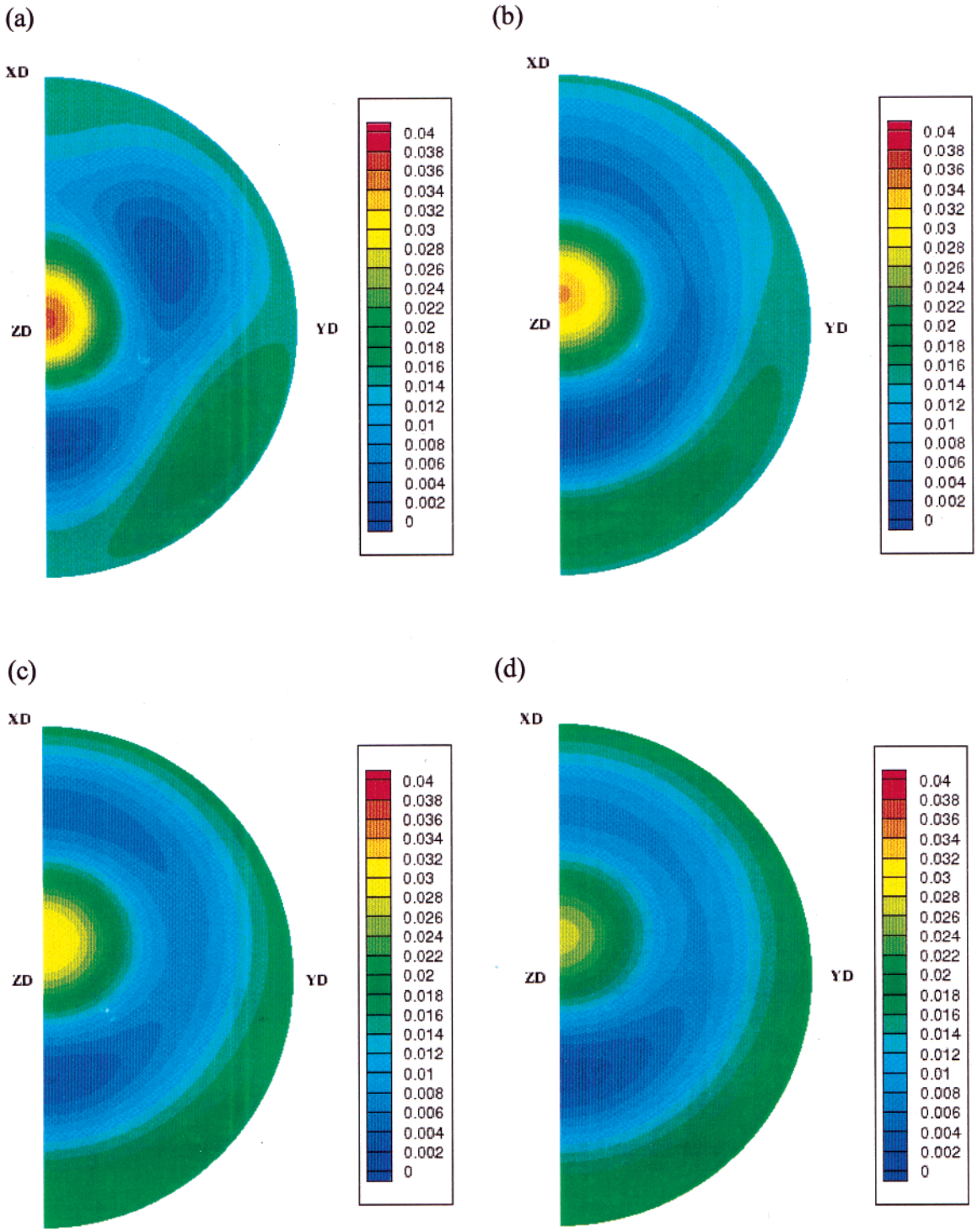

Figure 6. Best-fit orientation distribution functions $f(\Theta_M,\Phi_M)$ from NMR data for polystyrene samples sheared at We = 33 and allowed to relax for (a) 0, (b) 3, (c) 10, and (d) 30 s prior to quenching.

CODER NMR measurements on polystyrene samples that were first sheared in the melt state, allowed to relax for a short period of time, and then quenched to room temperature, as described previously.[24] The orientation distributions obtained, $f(\Theta_M,\Phi_M)$, describe the orientation of the repeat units (molecular reference frame) with respect to the shear flow field. Θ_M is the polar angle between the repeat unit axis (Z_M) and the shearing direction (Z_D), and Φ_M is the azimuthal angle of the projection of Z_M in the velocity gradient−neutral (X_D-Y_D) plane. Figure 6 shows analytical representations of the best fit orientation distributions for four samples sheared at 438 K and a Weissenberg number We = 33. These samples were allowed to relax for 0, 3, 10, or 30 s between the cessation of steady shear flow and quenching in liquid nitrogen.

In the single-chain SGMC simulations performed here, the local direction of the chain at each polystyrene repeat unit was defined by the vector between successive unsubstituted methylene carbons, as described above. The orientation distribution constraint obtained from NMR data on bulk samples and then imposed on the simulation implicitly includes contributions from interchain interactions in a dense, multichain environment; thus, these single-chain simulations are representative of conformations in a bulk phase. However,

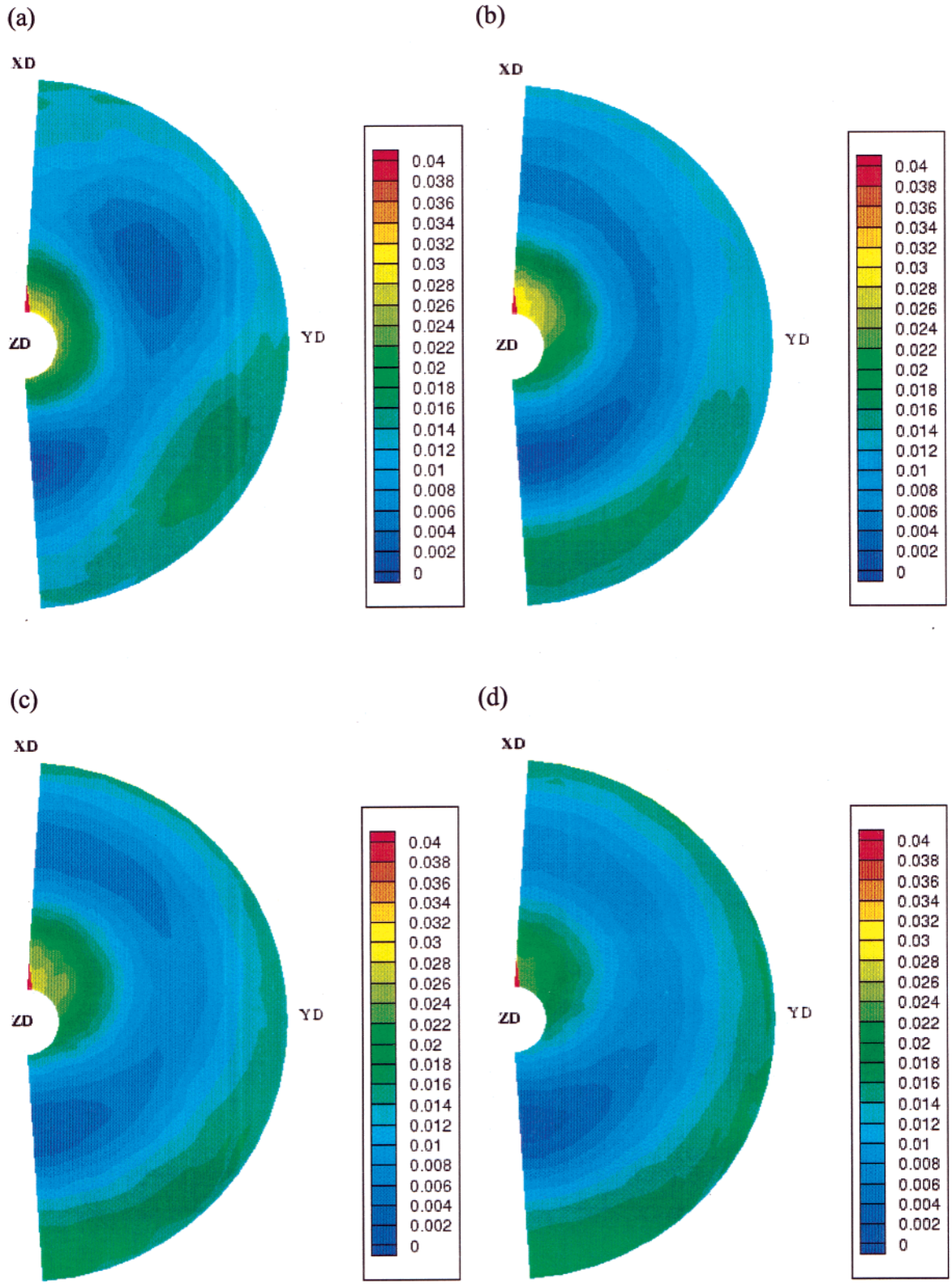

Figure 7. Monte Carlo representation of repeat unit axis orientation distribution functions corresponding to those introduced in Figure 6.

they do not account for possible intramolecular correlation of torsion angles along a chain that may arise due to specific packing interactions with neighboring chains. The orientation residual activity profile, $a^*(\cos\Theta_M,\Phi_M)$, was computed in 2500 discrete bins using 50 increments spanning $\cos\Theta_M$ in the interval $[-1,1]$ and 50 increments spanning Φ_M in the interval $[0,2\pi]$; it was calculated for every repeat unit of each chain simulated. Based on solution NMR measurements, the fraction of meso dyads used in the simulations was 0.67.[25] For simulation, we chose a chain of length 18 bonds (9 repeat units), approximately equal to the size of a statistical segment of polystyrene.[25] However, it should be noted that any chain length may be simulated with this method. At each MC step, an attempt was made to reptate a segment of the chain six bonds long; this choice

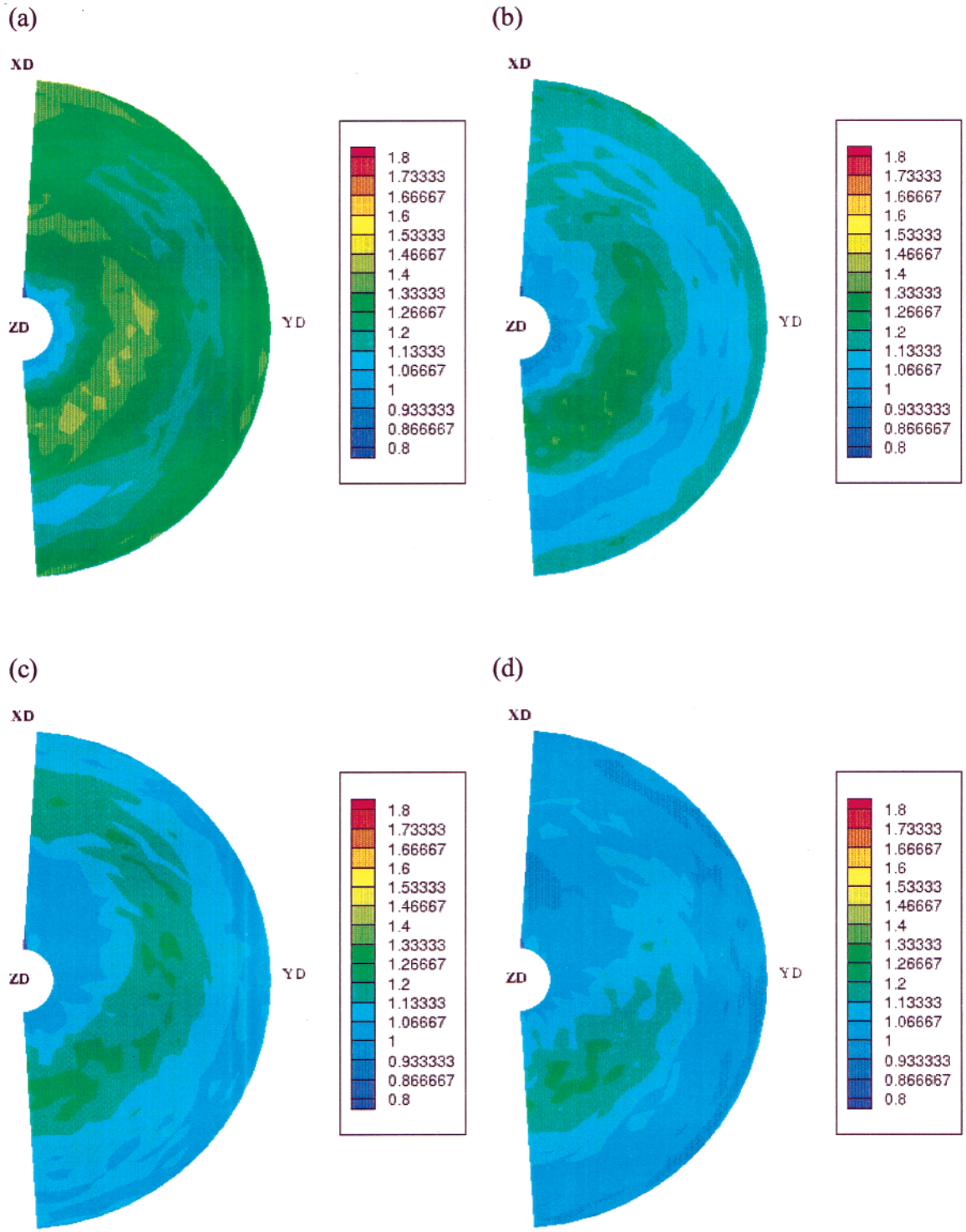

Figure 8. Residual activity profiles corresponding to the simulated orientation distribution functions in Figure 7.

yielded a good acceptance rate of moves (0.6−0.7) and ensured that an entire conformational update was accomplished every few MC moves. Iterations according to eq 11 to obtain the correct residual activity profile, $a^*(\cos \Theta_M, \Phi_M)$, were run for 10^5-10^6 MC moves and converged in 10−12 iterations.

The activity profiles were considered converged when the root-mean-square deviation between the Monte Carlo and analytical representations of the experimentally determined repeat unit orientation distributions ceased to change significantly between simulations, the moments of the tensor $\langle uu \rangle$ derived from the normalized end-to-end vector u did not change within statistical error, and the value of each point in the residual activity profiles did not change by more than 0.1% between iterations. The final simulations to collect data were run for 10^7 iterations to achieve adequately small statistical errors on the calculated moments of the orientation distributions of the statistical segments.

Results and Discussion

The resulting orientation distributions of the repeat units generated by the Monte Carlo method at a temperature of 438 K for the four sheared polystyrene samples are shown in Figure 7. The distribution functions are plotted in polar form, analogous to Figure 6,

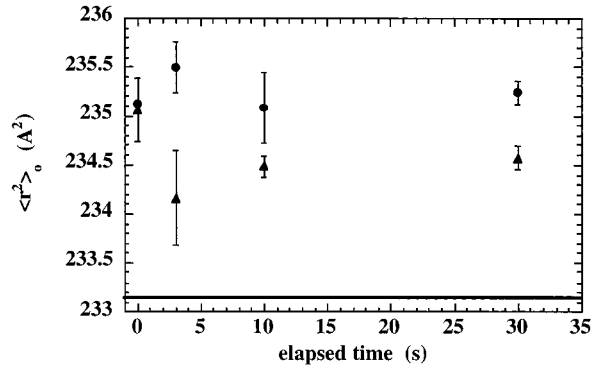

Figure 9. Variation of the unperturbed mean-squared end-to-end length of statistical segments of polystyrene following cessation of steady shear flow at 438 K for We = 33 (circles) and We = 3.3 (triangles). The solid line indicates the equilibrium (undeformed) value.

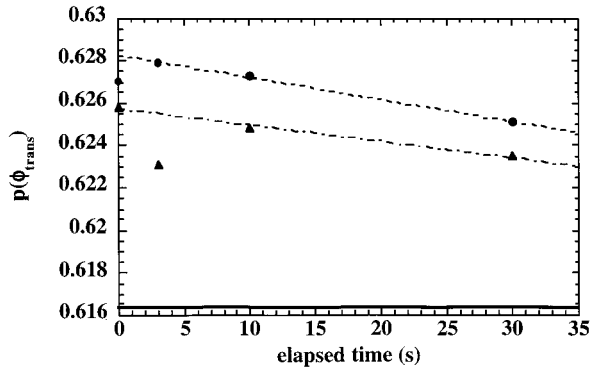

Figure 10. Probability of a backbone torsion angle being in the trans state [120°, 240°) as a function of time upon cessation of steady shear flow for We = 33 (circles) and We = 3.3 (triangles) at 438 K. The solid line indicates the equilibrium (undeformed) value.

with the radial axis being linear in Θ_M (not cos Θ_M) and the circumferential axis being linear in Φ_M. The transformation from cos Θ_M to Θ_M, plus the fact that we evaluated the distribution function at the midpoint of each bin, accounts for the lack of values at $\Phi_M = 0°$ and 180°, along the left edge of the plots in Figure 7.

It is clear by inspection that the repeat unit orientation distributions generated by the MC method are faithful representations of the experimentally measured distribution functions. The error between the simulated and the imposed distributions is generally on the order of 5%. The magnitude of this error is larger close to the location of the peak in the distribution function, at times approaching 15%. It should be possible to reduce this error systematically by running longer simulations and using a smarter scheme for updating the residual activity profile at each iteration.[26] However, for our current purpose of demonstrating the SGMC method, these refinements were not deemed necessary here.

Figure 8 shows the residual activity profiles for the four samples. The value of the residual activity is unity for the reference state, $\Theta_M = 0°$, by construction. The reported residual activity profiles do not extend all the way to $\Theta_M = 0°$, for the reasons cited above; nevertheless, the value of the residual activity is tending toward unity close to that point for all samples.

Figure 9 shows the unperturbed mean-squared end-to-end distance $\langle r^2 \rangle_0$ for the simulation of polystyrene 9-mers sheared at We = 33, as well as for simulations performed by using data from polystyrene samples sheared at We = 3.3. For comparison, the value of $\langle r^2 \rangle_0$ for a polystyrene 9-mer by conventional MC simulation (i.e., no orientational bias) is 233.3 ± 0.2 Å^2. Thus, in keeping with physical intuition, there is a small (ca. 1%) but statistically significant increase in the mean-squared end-to-end distance of the chain when sheared at higher We. From the data for $\langle r^2 \rangle_0$ it is not possible to pick out a significant trend in chain shape with increasing relaxation times between 0 and 30 s. However, evaluation of the asphericity $\langle b \rangle$ reveals that the 9-mers simulated here actually increase in asphericity with increasing relaxation time for both We numbers; this is counterintuitive. The asphericity we compute includes both internal orientation due to chain conformation and reorientation of the chain in the flow field. These results suggest that shearing in these experiments leads to extension of the chain segment (as indicated by $\langle r^2 \rangle_0$) with increasing We number but also to some misorientation of the chain segment, perhaps due to tumbling. Upon cessation of shearing, these 9-mers initially become more oriented on the time scale of seconds, followed by subsequent relaxation of the segments to their isotropic distribution. This initial increase in orientation could be due to cessation of tumbling dynamics or to intermolecular interactions.

A trend in conformation is more clearly seen in the fractions of torsions in the trans state, corresponding to ϕ values ranging from 120° to 240°, shown in Figure 10. At any given point during the relaxation process, the trans content of the segments in the samples processed at the higher We is greater than that for the segments in the samples processed at the lower We. Apart from the data points corresponding to the sample sheared at We = 33 and held for 0 s, and the sample sheared at We = 3.3 and held for 3 s, which are influenced by truncation error in the basis expansions,[24] the trans content decreases steadily toward the equilibrium value of 0.6163, as calculated for chains of the same length with no orientational bias applied. Therefore, as the chains are increasingly deformed at higher Weissenberg numbers, the chains elongate by rotation of the backbone torsions into the trans state, a process which reverses itself during stress relaxation.

Conclusions

The semigrand canonical Monte Carlo method for solving inverse problems is one in which ensembles whose properties satisfy known experimental data can be generated with the benefit of traditional interatomic potentials. In this paper, the orientational activity was combined with the conformational energy in the acceptance criteria for a MC move to simulate ensembles of polystyrene chains which exhibit an orientational bias.

Although the solution to the inverse problem may not be unique, it can be shown that the resulting collection of chain conformations is that which minimizes the Helmholtz free energy subject to agreement with the experimental data. The SGMC method is as much an analytical characterization tool for experimental data as it is a statistical thermodynamic technique. The SGMC method provides the best molecular model representation based on the data available that are used to constrain the simulation. Model representations may be further refined by using additional data sets, where available.

The SGMC modeling approach offers a new capability for simulation of molecular configurations in states far

from equilibrium. When supplied with appropriate sets of experimental data, this method may be used to generate quasi-static representations of the ensemble. If several sets of experimental data are collected in a time series, the succession of quasi-static representations is indicative of the evolution of the ensemble on an experimental time scale. As an illustration, this paper describes the analysis of conformational changes in polystyrene during stress relaxation following the cessation of steady shear flow over a period of 30 s. However, this technique may be applied to obtain insights at a molecular level of processes with much longer time scales. From data on the orientation distribution of repeat units, it is possible to infer the corresponding changes in the end-to-end distance and the population of rotational isomeric states.

Acknowledgment. This work was funded in part by grants from the 3M Company and by a Young Investigator Award of the National Science Foundation (CTS-9457111).

Appendix A. Selection of Bond Torsions

The Rapold and Suter polystyrene energy model[19] can be expressed as an a priori two-state probability distribution $p(\phi_i,\phi_{i+1})$ for finding a dyad with torsion angles ϕ_i and ϕ_{i+1}. The a priori one-state probability distribution $p(\phi_i)$ is related to the a priori two-state probability distribution by the conditional probability $q(\phi_{i+1}|\phi_i)$:[27]

$$p(\phi_i,\phi_{i+1}) = p(\phi_i)\, q(\phi_{i+1}|\phi_i) \tag{A-1}$$

The a priori two-state probability distribution is defined as

$$p(\phi_i,\phi_{i+1}) = \frac{e^{-\beta U(\phi_i,\phi_{i+1})}}{\int\int e^{-\beta U(\phi_i,\phi_{i+1})}\, d\phi_i\, d\phi_{i+1}} \tag{A-2}$$

The a priori one-state probability distribution is the integral of the two-dimensional a priori probability distribution over the second angle:

$$p(\phi_i) = \frac{\int e^{-\beta U(\phi_i,\phi_{i+1})}\, d\phi_{i+1}}{\int\int e^{-\beta U(\phi_i,\phi_{i+1})}\, d\phi_i\, d\phi_{i+1}} \tag{A-3}$$

Application of eq A-1 gives

$$q(\phi_{i+1}|\phi_i) = \frac{e^{-\beta U(\phi_i,\phi_{i+1})}}{\int e^{-\beta U(\phi_i,\phi_{i+1})}\, d\phi_{i+1}} \tag{A-4}$$

Hence, energy surfaces reported by Rapold and Suter[19] may be partitioned into a contribution from first-order interactions, which depends on the torsion of an individual bond and gives rise to $p(\phi_i)$, and a contribution arising from second-order interactions, which reflects also the value of the preceding torsion along the chain and is accounted for by $q(\phi_{i+1}|\phi_i)$:

$$U(\phi_i,\phi_{i+1}) = \left\{-\frac{1}{\beta}\ln \sigma_i\right\} + \left\{U(\phi_i,\phi_{i+1}) + \frac{1}{\beta}\ln \sigma_i\right\} \tag{A-5}$$

where

$$\sigma_i = \int e^{-\beta U(\phi_i,\phi_{i+1})}\, d\phi_{i+1} \tag{A-6}$$

The first term on the right-hand side of eq A-5 is that part of the energy of the dyad that is associated with the (already existing) torsion value at bond i, i.e., $U(\phi_i) = -(1/\beta)\ln \sigma_i$. The second term on the right-hand side of eq A-5 is the energy associated with adding the torsion ϕ_{i+1}, given that ϕ_i is already assigned, $U(\phi_{i+1}|\phi_i)$. This partitioning of the energy surfaces into these two contributions is shown in Figures 11 and 12 for both the meso and racemo dyads of polystyrene.

To configure a bond of type I (cf. Figure 4), the torsion value is selected from the a priori distribution for the bond (eq A-3). The pentane effect for conformations arising from the torsion pair (ϕ_{i-1},ϕ_i) centered on a

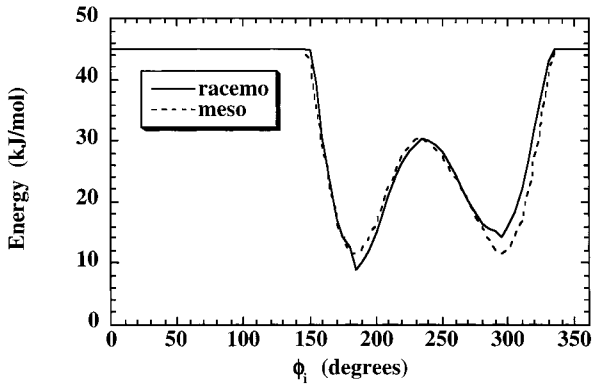

Figure 11. One-dimensional a priori energy profiles $U(\phi_i)$ for the racemo and meso dyads of 2,4-diphenylpentane.

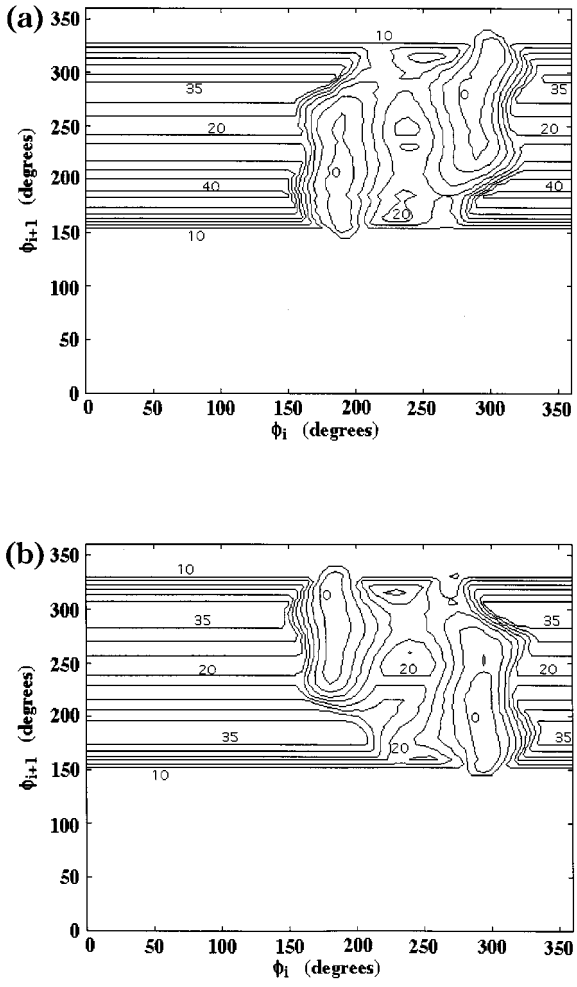

Figure 12. Conditional energy surface $U(\phi_{i+1}|\phi_i)$ for the (a) racemo and (b) meso dyad of 2,4-diphenylpentane. Contours are spaced every 5 kJ/mol with selected contours labeled.

substituted carbon is taken into account by assigning a statistical weight of zero[17,19] to the gg state; i.e., if the value of ϕ_{i-1} lies in the range [240°, 360°), the a priori probability of selecting ϕ_i in the range [240°, 360°) is set to zero. Also, any rotational isomeric $\bar{g}$ state is given a statistical weight of zero to satisfy the condition of microscopic reversibility.[28] To configure a bond of type $i + 1$ (cf. Figure 4), the torsion value is selected from the conditional probability distribution for that bond (eq A-4), given the value of the preceding torsion ϕ_i. This procedure is an extension of methods that have been described elsewhere[29] to simulate single chains within the rotational isomeric state (RIS) approximation.

Appendix B. Validation of Polystyrene Conformation Sampling

With this somewhat more complex chain model, several calculations were performed to validate the Monte Carlo code and the implementation of the energy partitioning described above.[25] We first compared the fraction of trans states from the original RIS model[19] at 300 K (meso: $f_{trans} = 0.831$; racemo: $f_{trans} = 0.489$) with the fraction of torsion angles in the interval [120°, 240°) from a standard canonical MC simulation of 2,4-diphenylpentane (meso: $f_{trans} = 0.834$; racemo: $f_{trans} = 0.491$) for both meso and racemic forms of 2,4-diphenylpentane. This agreement was deemed satisfactory for an ensemble of only 20 000 molecules.

As a second test, we simulated chains of length n from 100 to 500 bonds, having a fraction of meso dyads $f_m = 0.46$,[19] by using the standard, canonical MC simulation with a reptation move that attempted to reconfigure 1/3 of the chain at each move. From ensembles of 10 000 chains, we calculated the characteristic ratio:

$$C_n = \frac{\langle r^2 \rangle_0}{nl^2} \qquad \text{(B-1)}$$

where $\langle r^2 \rangle_0$ is the unperturbed mean-squared end-to-end distance of a chain comprised of n bonds of length l. Extrapolating to infinite chain length, we obtain the value of C_∞ to be 11.5. This is slightly higher than the value of 10.5 calculated by RIS in ref 19, but the difference is within one standard deviation for this small ensemble of chains. The value is within the range of experimental values cited for polystyrene.[19]

As demonstrated by Flory,[27] there are chain end effects that cause deviation in the distribution of torsion states for bonds near the end of a chain. Such deviations are usually limited to the first 2 or 3 bonds. The partitioning of the energy described in eq A-5 does not account for these end effects, nor for the fact that the first bond has no predecessor. Such end effects should be insignificant for chains of any appreciable length. Nevertheless, we can account for this end effect by estimating the appropriate distribution $p(\phi_1)$ for the first bond in the chain and then choosing subsequent torsions according to the conditional probability distribution based on $U(\phi_{i+1}|\phi_i)$. To estimate $p(\phi_1)$, we discretize the energy surfaces in Figure 5 in 5° increments (a total of 73 "isomeric states") and use the RIS formalism to construct a "pseudo-continuous" matrix of statistical weights. Using the equations of ref 27, we then estimate the a priori probability distribution for the first bond of 2,4,6-triphenylheptane in 5° increments. By drawing the first torsion of the first chain of the ensemble from this special distribution (all subsequent conformations being generated by reptation moves with torsion values selected according to the conditional probability distribution defined by the second-order interaction energy), a Monte Carlo simulation of 2,4,6-triphenylheptane was performed, and the torsional angle distributions for the individual torsions matched the two state RIS predictions.[19] This confirms that the partitioning of the energy set forth in eq A-5 is correct. Subsequent calculation of the characteristic ratio for syndiotactic and isotactic polystyrene chains with and without end effects confirmed that end effects are negligible for long chains. Further details of these validation procedures may be found in ref 25.

References and Notes

(1) *Structure and Properties of Oriented Polymers*; Ward, I. M., Ed. Applied Science: London, 1978.
(2) Kroger, M.; Luap, C.; Muller, R. *Macromolecules* **1997**, *30*, 526.
(3) Kroger, M.; Loose, W.; Hess, S. *J. Rheol.* **1993**, *37*, 1057.
(4) Khare, R.; de Pablo, J. J.; Yethiraj, A. *Macromolecules* **1996**, *29*, 7910.
(5) Andrews, N. C.; McHugh, A. J.; Schieber, J. D. *Macromol. Theory Simul.* **1998**, *7*, 19.
(6) Andrews, N. C.; McHugh, A. J.; Schieber, J. D. *J. Rheol.* **1998**, *42*, 281.
(7) Rapold, R. F.; Suter, U. W.; Theodorou, D. N. *Macromol. Theory Simul.* **1994**, *3*, 19.
(8) Robyr, P.; Gan, Z.; Suter, U. W. *Macromolecules* **1998**, *31*, 8918.
(9) Robyr, P.; Muller, M.; Suter, U. W. *Macromolecules* **1999**, *32*, 8681.
(10) McGreevy, R. L.; Pustzai, L. *Mol. Simul.* **1988**, *1*, 359.
(11) Rosi-Schwartz, B.; Mitchell, G. R. *Polymer* **1996**, *37*, 1857.
(12) Rosi-Schwartz, B.; Mitchell, G. R. *Polymer* **1994**, *35*, 5398.
(13) Mitchell, G. R.; Windle, A. H. *Polymer* **1984**, *25*, 906.
(14) Rutledge, G. C. *Phys. Rev. E* **2001**, *62*, 021111.
(15) Briano, J. G.; Glandt, E. D. *J. Chem. Phys.* **1984**, *80*, 3336.
(16) Yoon, D. Y.; Smith, G. D.; Matsuda, T. *J. Chem. Phys.* **1993**, *98*, 10037.
(17) Yoon, D. Y.; Sundararajan, P. R.; Flory, P. J. *Macromolecules* **1975**, *8*, 776.
(18) Mondello, M.; Yang, H.-J.; Furuya, H.; Roe, R.-J. *Macromolecules* **1994**, *27*, 3566.
(19) Rapold, R. F.; Suter, U. W. *Macromol. Theory Simul.* **1994**, *3*, 1.
(20) Smith, D. G.; Ayyagari, C.; Jaffe, R. L.; Pekny, M.; Bernarbo, A. *J. Phys. Chem. A* **1998**, *102*, 4694.
(21) We adopt the convention where the trans conformation is defined as $\phi = 180°$, in contrast to the convention of Flory et al.,[22] $\phi = 0°$, adopted by Rapold and Suter.[19]
(22) Flory, P. J.; Sundararajan, P. R.; DeBolt, L. C. *J. Am. Chem. Soc.* **1974**, *96*, 5015.
(23) The stereochemical configuration of the polystyrene chain is specified by designating skeletal bonds as l or d when viewed in the same direction from the substituted carbon to the methylene carbon. A meso dyad is composed of two bonds of alternating designation, ld or dl, while a racemo dyad is composed of two identical enantiomeric bonds, dd or ll. The enantiomeric label of skeletal bonds is always different for bonds on either side of the substituted carbon. A torsion about a d bond is positive in a right-handed sense, and a torsion about an l bond is positive in a left-handed sense.
(24) Colhoun, F. L.; Armstrong, R. C.; Rutledge, G. C. *Macromolecules* **2001**, *34*, 6670.
(25) Colhoun, F. L. Relaxation of Processing Induced Orientation in Polymer Melts. Ph.D. Thesis, M.I.T., 2000.
(26) Bathe, M.; Rutledge, G. C. *Biophys. J.*, submitted.
(27) *Statistical Mechanics of Chain Molecules*; Flory, P. J., Ed.; Hanser: New York, 1969.
(28) This is implemented by assigning these states energies of 200 kJ/mol, which translates into a probability of zero within computer roundoff error.
(29) *Conformational Theory of Larger Molecules: The Rotational Isomeric State Model in Macromolecular Systems*; Mattice, W. L., Suter, U. W., Eds.; Wiley and Sons: New York, 1994.

MA020347H